Quaternary Science Reviews 29 (2010) 3317–3326

Contents lists available at ScienceDirect

Quaternary Science Reviews

journal homepage: www.elsevier.com/locate/quascirev

Geochemical evidence for the provenance of middle Pleistocene loess deposits in southern China

Qingzhen Hao [a,*], Zhengtang Guo [a], Yansong Qiao [b,c], Bing Xu [a], Frank Oldfield [d]

[a] Key Laboratory of Cenozoic Geology and Environment, Institute of Geology and Geophysics, Chinese Academy of Sciences, Beijing 100029, China
[b] Institute of Geomechanics, Chinese Academy of Geological Sciences, Beijing 100081, China
[c] Key Laboratory of Neotectonic Movement & Geohazard, Beijing 100081, China
[d] School of Environmental Sciences, University of Liverpool, Liverpool, L69 7ZT, UK

ARTICLE INFO

Article history:
Received 14 April 2010
Received in revised form
3 August 2010
Accepted 4 August 2010

ABSTRACT

The provenance of middle Pleistocene loess in the middle and lower reaches of the Yangtze River, the most intensively investigated loess deposits outside the Loess Plateau region in China, remains controversial. Identification of the provenance will provide crucial insight into the environmental implications of this valuable sedimentary archive, and into the potential role of the East Asian winter monsoon in transporting the dust from deserts in the Asian interior. In this study, geochemistry was used to compare the provenance of loess in the lower reaches of the Yangtze River in southern China with that inferred for loess deposits on the Loess Plateau in northern China. Compared with samples from the Loess Plateau, the <20 μm fraction in the loess deposits of southern China has higher TiO_2/Al_2O_3, Zr/Nb, Zr/Al, Zr/Ti, Zr/Hf, Y/Al and La_N/Sm_N ratios, and lower Eu/Eu*, Th/Nb, Y/Nb and Al/Nb ratios. The clear distinction in immobile element ratios between samples from the two regions indicates that the loess deposits in the two regions have different provenances. The inferred difference in source area is also supported by variations in the major element composition of bulk samples obtained in this study and collected from published data. These lines of evidence indicate that the deserts in the Asian interior are not the primary provenance for the southern loess. It is suggested that the adjacent floodplains to the north of Yangtze River are the dominant dust sources, and the occurrence of sustained loess deposits in the lower reaches of the Yangtze River, currently an area of northern subtropical climate, is an indication of local aridification and strengthened winter monsoon activity during glacial periods as a regional response to the Middle Pleistocene climate transition around 0.8 Ma. The role of the East Asian winter monsoon in transporting the dust from northern deserts to southern China has been overestimated in previous studies.

1. Introduction

Thick loess deposits cover not only the Chinese Loess Plateau (CLP) in north-central China, but are distributed in northwestern, eastern and southern China (Liu, 1985) (Fig. 1a). In recent years, increasing interest has been focused on the loess outside the CLP in order to derive environmental information from a wider area. Among these, the most extensively investigated are the southern loess deposits of middle Pleistocene age, which are widely distributed in the middle and lower reaches of the Yangtze River (Liu, 1985; Huang et al., 1988) (Fig. 1), because well preserved terrestrial climate records with a long time span are scarce in subtropical regions. Up to now, the grain-size characteristics (Li et al., 1997, 2001; Qiao et al., 2003), clay mineral assemblage (Shi et al., 2005), chemical weathering (Yang et al., 2004; Chen et al., 2008), lipid biomarkers (Xie et al., 2003) and environmental magnetism (Zhang et al., 2007, 2009) have been investigated in order to reconstruct middle Pleistocene paleoenvironments in this northern subtropical region.

The occurrence of continuous loess deposits reflects an important environmental change in the source and/or deposition regions (Pye, 1995). Although the eolian origin has been well accepted (Hsü, 1936; Liu, 1985; Yang et al., 1991; Wu et al., 1992; Li et al., 1997, 2001; Qiao et al., 2003), the source of the southern loess remains controversial. The predominant and traditional view, based on sediment distribution (Liu, 1985) (Fig. 1a) and grain-size features (Liu, 1985; Yang et al., 1991; Li et al., 1997, 2001), is that the southern loess materials were mainly blown from the deserts in northern

* Corresponding author. Tel.: +86 10 82998395; fax: +86 10 62010846.
E-mail address: haoqz@mail.iggcas.ac.cn (Q. Hao).

0277-3791/$ – see front matter © 2010 Elsevier Ltd. All rights reserved.
doi:10.1016/j.quascirev.2010.08.004

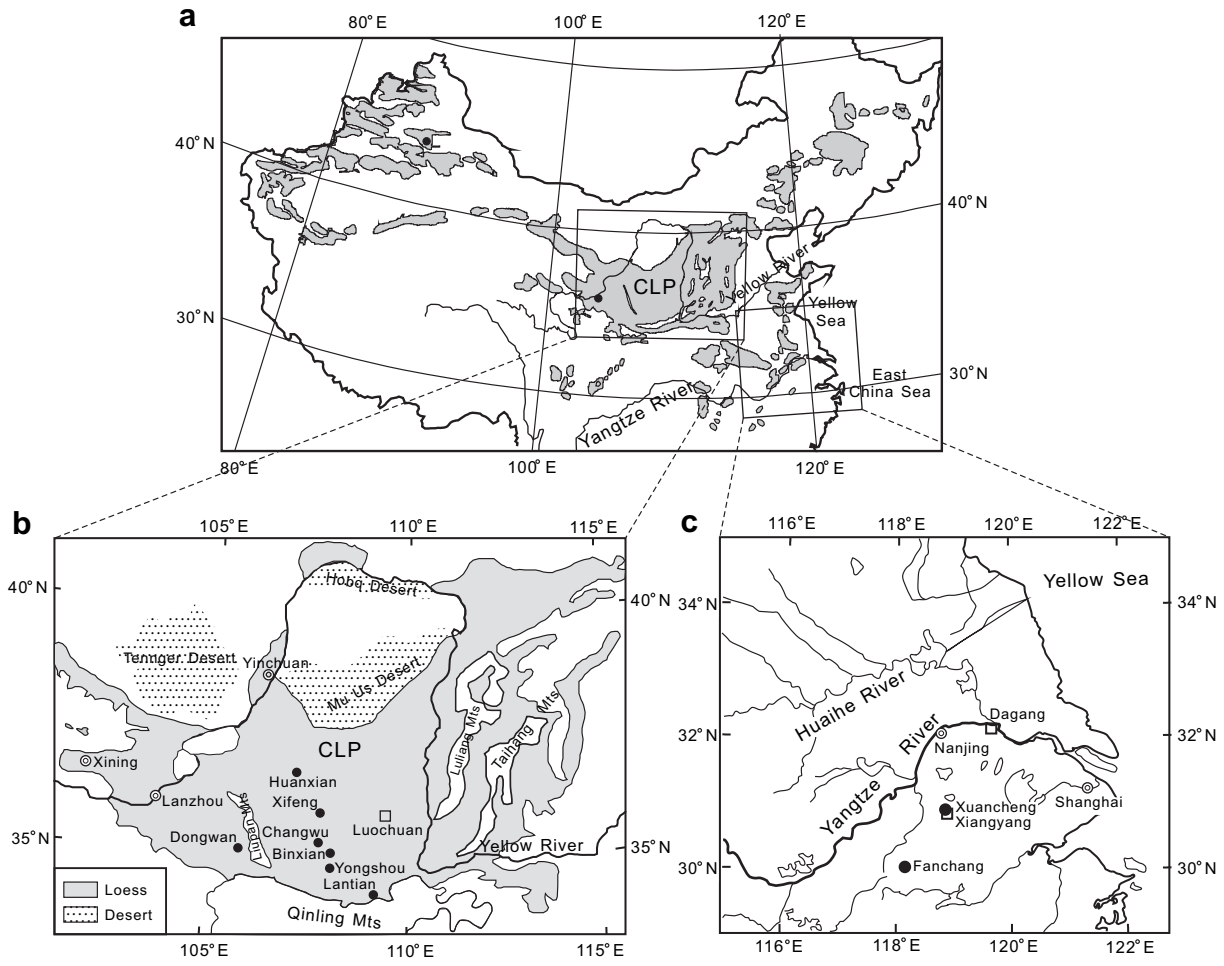

Fig. 1. Location map showing loess distribution in China and the location of the sites mentioned. (a) Distribution map of loess in China, (b) Map of the Chinese Loess Plateau (CLP) and (c) the *Xiashu* loess sections in the lower reaches of the Yangtze River. The solid circles refer to the sampling sites and open squares to the sites mentioned. The east–west trending Qinling Mountains are the traditional dividing line between temperate northern China and subtropical southern China.

China, as is the case with the well-documented loess on the CLP. Several other studies have proposed that fine-grained fluvial deposits in local river valleys and/or lake beds, exposed during glacial times, made an important contribution (Wu et al., 1992; Qiao et al., 2003), since the deposits contain significant proportions of particles larger than 32 μm (Qiao et al., 2003) which are usually unlikely to be transported for a long distance by wind. The different views on the provenance of the southern loess have led to contrasting environmental interpretations. The former view implies that the formation of the southern loess was a consequence of increasing aridity in the northern dust source area coupled with intensified East Asian winter monsoon activity, linked to uplift of the Tibetan Plateau and the consequent southward displacement of Northern Hemisphere westerlies (e.g. Liu, 1985; Yang et al., 1991). The latter interpretation considers the occurrence of the southern loess to be an indicator of aridification in nearby subtropical environments during glacial times (e.g. Qiao et al., 2003). Therefore, identification of the provenance of the southern loess could provide new insights into the environmental implications of the sedimentary records and the driving factors in climate change in the northern subtropical area of China.

The role of dust in climate change has become a major focus of Earth system modeling research (e.g. Kohfeld and Harrison, 2001). Atmospheric dust is an important feedback in the climate system, potentially affecting the radiative balance and chemical composition of the atmosphere and providing nutrients to terrestrial and marine ecosystems (e.g. Kohfeld and Harrison, 2001). Loess deposits provide a record of past atmospheric dust deposition that constitutes an important constraint on Earth system models incorporating past dust cycles (e.g. Kohfeld and Tegen, 2007). Identification of loess sources in China will provide important information on dust emission, transport and deposition in Asia (Kohfeld and Harrison, 2003) and improve our understanding of the potential role of the East Asian winter monsoon in spreading the desert dusts in the Asian interior beyond the limits of the CLP.

The chemically immobile major (e.g. Al and Ti), and trace elements (e.g. rare earth elements (REE), Y, Th, Sc, Zr, Hf and Nb) have great potential for determining the provenance of clastic sediments (Taylor and McLennan, 1985; Bhatia and Crook, 1986; McLennan et al., 1993), because they maintain invariant ratios during post-depositional chemical weathering. This approach has been used successfully in the provenance identification of eolian deposits in various regions (Muhs et al., 1996, 2008; Reheis et al., 2002; Sun, 2002; Guan et al., 2008).

In this paper, the relatively immobile major and trace element compositions are compared between a typical southern loess section and those from the CLP, with a view to providing geochemical constraints on the source of the southern loess. The comparison is mainly based on the geochemistry of the <20 μm fraction of the samples. The major element composition of the bulk

samples on an NW-SE transect across the CLP and southern sites is also analyzed to establish whether the spatial changes of SiO_2/Al_2O_3, mainly related to sedimentary differentiation in the present study, are consistent with the notion that the southern loess materials are derived from northern deserts.

2. Materials and methods

2.1. Materials

The Xuancheng (XC) section (118°51′E, 30°54′N) is one of the typical loess sections in the lower reaches of the Yangtze River (Yang et al., 1991; Zhao and Yang, 1995; Qiao et al., 2003) (Fig. 1c). This section is lithologically divided into three units: cultivated soil (0–0.2 m), the so-called *Xiashu* loess-soil sequence (0.2–4.0 m) and the so-called Vermiculated Red Soil (VRS) (4.0–10.0 m) that is much more strongly weathered than the soil layers represented in the *Xiashu* formation. Paleomagnetic dating recognized the Brunhes/Matuyama (B/M) reversal boundary within the lower part of the VRS (Qiao et al., 2003), consistent with the previous ESR results (Zhao and Yang, 1995). Microscopic and sedimentologic investigations reveal that eolian deposition started at depth of 9.1 m, dated to ca 0.85 Ma, in the section (Qiao et al., 2003). Eight samples were taken from the eolian part of this section, five from the upper *Xiashu* loess and three from the lower VRS layers. The CLP samples come from Xifeng and Dongwan (Fig. 1b): five Pleistocene loess samples from the Xifeng section (Guo et al., 2000) and one from the late Pleistocene loess unconformably overlying the late Neogene Dongwan sequence on the western CLP (Hao and Guo, 2004). Five samples from the upper part (4.7–2.6 Ma) of the Xifeng Red-Earth section (Guo et al., 2001) were also used for comparison. These Pliocene samples are finer-grained than Pleistocene loess, providing a basis for assessing the geochemical composition of loess from the CLP, with similar grain-size distributions to the Xuancheng loess. The <20 μm fraction (see Section 2.2) of the above samples has been used for major and trace element analysis.

The major element abundance in bulk samples has also been analyzed to provide information on spatial changes in the SiO_2/Al_2O_3 ratio related to sedimentary sorting. These samples include: ten bulk samples from southern China, five from XC, and five from Fanchang (FC, 118°09′E, 30°03′N), a parallel section to XC (Qiao et al., 2003) (Fig. 1c); twelve samples from the CLP, taken from Last Glacial Maximum loess L1LL1 and Last Interglacial Optimum soil S1 from six sites in an NW-SE transect (Fig. 1b). These are the same samples as those used in Fig. 5 of Hao and Guo (2005).

2.2. Fine fraction extraction

We use the <20 μm fraction to determine dust provenance in order to avoid the effects of particle size on the geochemical and mineralogical components (cf. Sun, 2002). The <20 μm fraction was pipetted from suspension based on Stoke's law. According to Tsoar and Pye (1987), only dust particles finer than 20 μm can be transported in long-term suspension over a great altitudinal range and long distances. Use of the <20 μm fraction removes any geochemical contribution from coarse particles mainly derived from local loess deposition sites. Moreover, the <20 μm fraction accounts for over 80% of the mass of the XC samples (Qiao et al., 2003) and the Pliocene Red Earth samples from Xifeng (Guo et al., 2001), and over 40% of the Pleistocene loess in this study. It therefore represents the major component for most of the samples considered here.

2.3. Geochemical analysis

All the samples were finely ground in an agate mortar before acid dissolution. Major element abundances were determined by XRF using a Rigaku 3080E in the National Research Center of Geoanalysis, Chinese Academy of Geological Sciences. Analytical uncertainties are ±2% for all major elements except for P_2O_5 and MnO (up to ±10%). Loss on ignition (LOI) was obtained by weighing after 1 h of heating at 950 °C.

The trace element composition of the <20 μm fraction was determined using an ICP-MS (ELEMENT, Finnigan MAT) at the Institute of Geology and Geophysics, Chinese Academy of Sciences. The samples were digested in HNO_3 (1:1) and HF under high temperature and pressure using a two-step procedure as detailed in Ding et al. (2001) in order to ensure complete refractory mineral dissolution. The analytical uncertainties are less than 10% for most of the trace elements.

3. Major and trace element geochemistry

3.1. Geochemistry of the fine fraction (<20 μm)

3.1.1. Major element geochemistry

The <20 μm fraction of the loess samples from the XC section and the CLP has different major element abundances, as summarized in Table 1. Major element abundances in the studied samples are rather uniform for each site, reflecting the well-mixed nature of the sediments. Compared with those from the CLP, the XC loess samples have a higher SiO_2 and TiO_2 content and lower Al_2O_3, Fe_2O_3, MgO, CaO, Na_2O, K_2O and P_2O_5 content. The difference in MnO concentration between the two regions is variable.

The TiO_2/Al_2O_3 ratio is very useful in provenance identification for various sediments (e.g. Sheldon and Tabor, 2009) because Ti content may be quite variable among different types of rocks, even when Al content remains relatively constant (Li, 2000). Both Al and Ti have the lowest solubility in natural water of all the major elements (Broecker and Peng, 1982; Sugitani et al., 1996). The K_2O/Al_2O_3 ratio in sediments is generally used as an index of chemical maturity, but can also be used as an indicator of the original composition of sediments in the early stages of chemical weathering characterized by Ca and Na removal (Cox et al., 1995), because the K_2O/Al_2O_3 ratio is markedly different in various feldspars, mica and clay minerals (Deer et al., 1966; Cox et al., 1995). K-feldspar is more resistant to chemical weathering than plagioclase, and during

Table 1
Mean concentrations (wt %) of major elements in the <20 μm fraction of loess deposits from southern China and the Chinese Loess Plateau, recalculated on a volatile-free basis (for locations see Fig. 1).

Oxide	Xuancheng		Xifeng		Dongwan Loess ($n = 1$)
	Xiashu loess ($n = 5$)	VRS ($n = 3$)	Loess ($n = 5$)	Red Earth ($n = 5$)	
SiO_2	70.52 ± 2.66	71.78 ± 0.68	63.07 ± 0.94	63.17 ± 0.54	63.35
Al_2O_3	17.84 ± 1.75	17.91 ± 1.04	18.38 ± 0.51	18.54 ± 0.39	18.13
Fe_2O_3	6.76 ± 0.95	6.46 ± 0.33	7.86 ± 0.25	7.79 ± 0.17	7.77
MnO	0.13 ± 0.04	0.03 ± 0.02	0.14 ± 0.03	0.12 ± 0.01	0.13
MgO	0.84 ± 0.15	0.65 ± 0.03	3.53 ± 0.22	3.82 ± 0.23	3.20
CaO	0.12 ± 0.02	0.13 ± 0.01	1.27 ± 0.18	1.14 ± 0.03	1.44
Na_2O	0.26 ± 0.1	0.20[a]	1.26 ± 0.19	0.94 ± 0.2	1.42
K_2O	2.24 ± 0.17	1.82 ± 0.06	3.48 ± 0.11	3.47 ± 0.09	3.56
TiO_2	1.23 ± 0.08	1.15 ± 0.06	0.84 ± 0.02	0.85 ± 0.01	0.84
P_2O_5	0.08 ± 0.01	<0.01	0.17 ± 0.02	0.16 ± 0.02	0.17
Total	100	100	100	100	100
LOI	5.88 ± 0.6	5.94 ± 0.37	5.37 ± 0.47	5.51 ± 0.36	5.49

[a] The Na_2O content of two samples was not detectable (<0.05%).

the weathering of K-bearing silicates, part of the K is tightly bound in the illite clay lattice, thus making it less mobile than Na in the weathering profiles.

The XC loess and the CLP samples are clearly distinguished from one another using a plot of K_2O/Al_2O_3 vs. TiO_2/Al_2O_3 (Fig. 2). The XC loess is characterized by high TiO_2/Al_2O_3 and low K_2O/Al_2O_3 values. The lower values of K_2O/Al_2O_3 ratio for the XC deposits may be partly caused by post-depositional weathering; however, the distinct envelopes of values for TiO_2/Al_2O_3 in the two regions provide the first evidence for their different sources.

3.1.2. Trace element geochemistry

The trace element (including REE) concentrations of the <20 μm fraction of the loess samples also show differences between the XC section and the CLP (Table 2). As in the case of the major elements, the concentrations of trace elements and REE are rather uniform for the deposits at each site. Compared with the loess in northern China, the <20 μm fraction of the XC samples has higher concentrations of Y, Nb, Zr, Hf, Ta and all REEs, lower concentrations of Sc, Rb, Sr, Cs, Ba, Pb, Bi, etc., and similar concentrations of Th, U and Ga.

The chondrite-normalized REE distribution patterns for the southern and northern loess (Fig. 3) are rather uniform in each region, characterized by steep light-REE (LREE) and relatively flat heavy-REE (HREE) patterns, and by persistent negative Eu anomalies. The distribution patterns are similar to those of UCC (Taylor and McLennan, 1985).

REEs are widely used in the provenance characterization of various sediments (Taylor and McLennan, 1985; McLennan, 1989; McLennan et al., 1993; Yang et al., 2007b; Muhs et al., 2008). LREE/HREE and La_N/Yb_N (chondrite-normalized data) reflect the fractionation of HREE and LREE. La_N/Sm_N and Gd_N/Yb_N are indicators of LREE and HREE differentiation, respectively. The Eu anomaly is quantified by Eu/Eu*, where Eu is Eu_N, and Eu* is $(Sm_N \times Gd_N)^{0.5}$. The plots of these REE distribution parameters are given in Fig. 4. These plots also show the different REE compositions for the <20 μm fraction between the XC and CLP samples. The XC fine fraction generally has lower Eu/Eu*, higher La_N/Sm_N, and a wider range of values for Gd_N/Yb_N and La_N/Yb_N.

The above differences in REE properties may mainly reflect the changes in sedimentary protoliths. Although REEs are usually relatively immobile elements, there is evidence showing that HREE are mobilized to a greater extent than are the LREE, and that strong weathering leads to a decrease in La_N/Sm_N values, and an increase in La_N/Yb_N and Gd_N/Yb_N values (e.g. Gouveia et al., 1993; Galan et al., 2007). If the XC loess originated from northern deserts, and their REE compositions were severely altered by the post-depositional weathering, we would see decreased La_N/Sm_N values, and increased La_N/Yb_N and Gd_N/Yb_N values. However, the increased La_N/Sm_N values and comparable or lower La_N/Yb_N and Gd_N/Yb_N values of XC samples run contrary to the expected weathering effect on the fractionation of REE (Gouveia et al., 1993; Galan et al., 2007). Y has similar geochemical behaviors to HREE (Taylor and McLennan, 1985). The overall higher Y/Al values for the XC samples also suggest enrichment rather than depletion for the HREE (see Section 3.1.3). As for europium, the difference in Eu/Eu* values in eolian dust deposits is attributed to changes in dust provenance (Gallet et al., 1998; Yang et al., 2007a; Muhs et al., 2008). The slightly negative Eu anomaly in the XC loess may reflect a low content of Eu-rich Ca-plagioclase in the source material.

Trace elements La, Y, Th, Zr, Hf, Nb, Sc, etc. are thought to be the most suitable for provenance determinations because of their relatively low mobility during sedimentary processes (Holland, 1978). These elements are incorporated into clastic sedimentary rocks during weathering and transportation with little alteration and thus would reflect the signature of the parent material (McLennan et al., 1983; Bhatia and Crook, 1986). Kurtz et al. (2000) demonstrated that Nb and Ta are virtually immobile, even in strongly weathered soils with total Si depletion. Kahmann et al.

Table 2
Mean concentrations (ppm) of trace elements in the <20 μm fraction of loess deposits from southern China and the Chinese Loess Plateau (for locations see Fig. 1).

Element	Xuancheng		Xifeng		Dongwan Loess ($n = 1$)
	Xiashu loess ($n = 5$)	VRS ($n = 3$)	Loess ($n = 5$)	Red Earth ($n = 5$)	
Li	63.6 ± 3.5	49.5 ± 19.9	54.9 ± 3.6	60.7 ± 2.2	58.0
Be	2.59 ± 0.24	1.84 ± 0.05	2.64 ± 0.09	2.78 ± 0.04	2.93
Sc	13.9 ± 1.4	13.5 ± 2.1	16.8 ± 1.4	17.8 ± 0.5	18.8
V	121 ± 14	116 ± 4	117 ± 5	124 ± 9	121
Co	17.2 ± 4.2	7.5 ± 2.5	20.7 ± 2.6	19.3 ± 2.4	21.2
Ga	21.4 ± 1.3	20.1 ± 0.5	21.3 ± 1.0	22.2 ± 0.7	22.3
Rb	119 ± 21	114 ± 9	125 ± 15	137 ± 9	156
Sr	52.7 ± 3.7	50.1 ± 1.0	113 ± 13	104 ± 8	124
Y	29.5 ± 5.0	26.9 ± 0.3	22.6 ± 2.2	23.1 ± 1.1	27.4
Zr	238 ± 39	251 ± 24	151 ± 3	152 ± 6	160
Nb	25.0 ± 1.3	24.7 ± 1.8	16.3 ± 0.4	16.6 ± 0.2	17.1
Cs	10.1 ± 1.0	11.5 ± 1.1	11.9 ± 0.8	13.2 ± 0.3	13.7
Ba	489 ± 33	352 ± 16	578 ± 54	543 ± 22	631
La	44.4 ± 7.3	39.4 ± 5.0	33.4 ± 2.6	34.5 ± 1.8	40.0
Ce	89.3 ± 13.0	72.6 ± 20.4	66.8 ± 4.2	67.6 ± 3.0	78.0
Pr	9.97 ± 1.45	8.42 ± 1.19	7.38 ± 0.58	7.64 ± 0.35	8.88
Nd	36.0 ± 6.3	30.7 ± 5.3	28.0 ± 2.1	28.9 ± 1.7	33.4
Sm	6.50 ± 1.12	5.30 ± 1.00	5.27 ± 0.46	5.44 ± 0.32	6.13
Eu	1.20 ± 0.22	0.99 ± 0.22	1.02 ± 0.10	1.05 ± 0.07	1.22
Gd	5.23 ± 0.91	4.55 ± 0.83	4.37 ± 0.38	4.51 ± 0.28	5.26
Tb	0.88 ± 0.16	0.80 ± 0.14	0.75 ± 0.08	0.75 ± 0.02	0.89
Dy	5.16 ± 0.85	4.63 ± 0.48	4.42 ± 0.43	4.32 ± 0.17	5.30
Ho	1.01 ± 0.15	0.96 ± 0.06	0.89 ± 0.08	0.87 ± 0.03	1.05
Er	2.84 ± 0.44	2.70 ± 0.23	2.52 ± 0.23	2.51 ± 0.09	2.95
Tm	0.44 ± 0.06	0.43 ± 0.03	0.39 ± 0.04	0.39 ± 0.01	0.46
Yb	2.90 ± 0.37	2.85 ± 0.09	2.51 ± 0.22	2.48 ± 0.06	2.94
Lu	0.44 ± 0.05	0.43 ± 0.01	0.38 ± 0.04	0.37 ± 0.00	0.43
Hf	6.53 ± 1.04	7.14 ± 0.11	4.69 ± 0.09	4.55 ± 0.21	4.87
Ta	1.87 ± 0.13	1.89 ± 0.05	1.25 ± 0.04	1.29 ± 0.04	1.35
Tl	0.66 ± 0.01	0.71 ± 0.03	0.75 ± 0.04	0.76 ± 0.03	0.81
Pb	29.3 ± 1.6	24.7 ± 2.8	35.7 ± 1.9	32.0 ± 0.8	34.5
Bi	0.36 ± 0.04	0.37 ± 0.02	0.50 ± 0.02	0.48 ± 0.01	0.50
Th	15.8 ± 1.2	14.5 ± 1.5	13.9 ± 1.3	14.0 ± 0.4	16.1
U	3.18 ± 0.29	3.24 ± 0.45	2.97 ± 0.72	2.92 ± 0.08	2.73

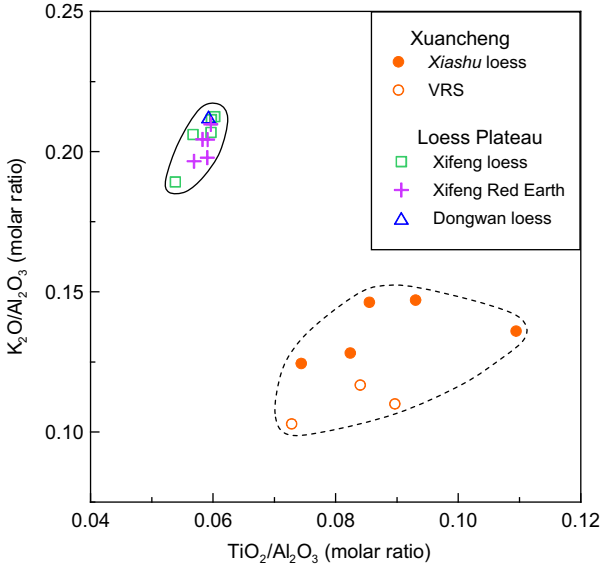

Fig. 2. Plot of of K_2O/Al_2O_3 vs. TiO_2/Al_2O_3 for the <20 μm fraction of loess deposits from Xuancheng in southern China and the CLP in northern China.

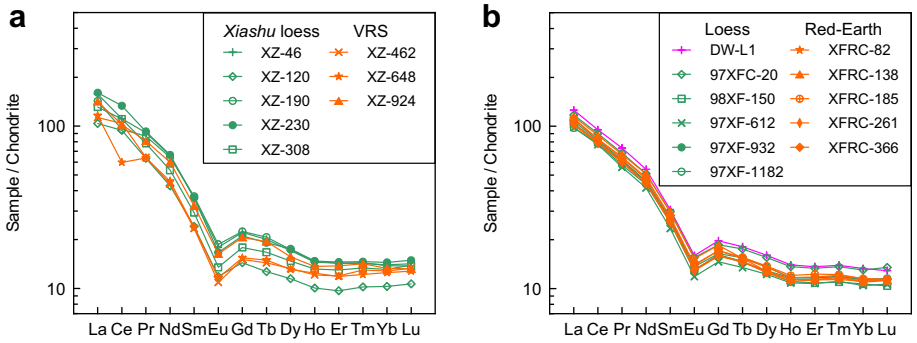

Fig. 3. Chondrite-normalized REE distribution patterns for the <20 μm fraction of loess deposits from Xuancheng in southern China (a) and the CLP in northern China (b).

(2008) demonstrated that Nb has the highest positive cross-correlation coefficients with other relatively immobile elements, e.g. La, Y, Th, Zr, Hf, in paleosols, also suggesting their similar behaviors in sedimentary processes. These results further support the value of these elements in provenance determination. In terms of geochemical behavior, Th displays coherent behavior with REE, whilst Y mirrors the heavy REEs. Because the fractionation of Nb and Ta from REEs has provided crucial constraints on crust-mantle differentiation and crustal growth processes (Barth et al., 2000 and references therein), the ratios La/Nb, Y/Nb, Th/Nb may allow us to discriminate provenance linked to different parent rocks in different tectonic settings. Zr and Hf are enriched in zircon, one of the ultra stable minerals frequently used in sediment source discrimination. Thus, Zr/Hf at least partly reflects the compositional changes of zircon.

The XC loess samples are clearly separated from the CLP ones by element ratio plots of La/Nb vs. Th/Nb, Zr/Nb vs. Hf/Nb and Y/Nb vs. Zr/Hf (Fig. 5a). Compared to those on the CLP, the XC loess samples have generally higher values for Zr/Nb and Zr/Hf, and lower values for the Th/Nb and Y/Nb ratios. A positive correlation of Zr/Nb vs. Hf/Nb is to be expected, since Zr and Hf have similar geochemical behavior and both are strongly enriched in zircon. The clear off-setting of the XC loess samples from the CLP ones in the plot of Zr/Nb vs. Hf/Nb and the different values in Zr/Hf suggest different compositions for the zircons in the deposits between the two regions.

The difference in composition of loess between the two regions is also seen in ternary diagrams of La–Th–Sc (Taylor and McLennan, 1985; Bhatia and Crook, 1986) and Zr/10-Th–Sc (Bhatia and Crook, 1986), illustrated in Fig. 5b. These ternary diagrams have been used successfully in the provenance identification of eolian deposits (e.g. Muhs et al., 2008). The XC samples are offset from those of the CLP ones, being located further away from the Sc apex in the two diagrams.

3.1.3. Element ratios between major and trace elements

Fralick and Kronberg (1997) presented an example of using element ratios between major (Al, Ti) and trace elements (Nb, Zr) to discriminate the provenance of clastic sand-sized sedimentary rocks. The Y/Al ratio is also used to indicate partial removal of Y from the sediment system. These plots for our data in Fig. 6 indicate again distinctly different compositions for the southern and northern loess deposits. The XC samples have overall higher Y/Al values, indicating the enrichment rather than depletion of Y.

3.2. Spatial changes in the SiO_2/Al_2O_3 ratio in bulk samples

Sedimentary sorting leads to variations in the grain-size of sediments linked to the distance of transportation. This, in turn, leads to grain-size dependent changes in mineral assemblages and element ratios. Si and Al remain unchanged in the weathering of loess deposits on the CLP (Gallet et al., 1996; Chen et al., 2001; Jahn et al., 2001). The SiO_2/Al_2O_3 ratio is proportional to particle size in the <50 μm fractions of loess deposits and has been proposed as a proxy to reflect the grain-size of original eolian particles, because weathering-resistant quartz as a major component in loess detrital minerals tends to be enriched in the coarser fractions (Peng and Guo, 2001), whereas Al tends to be enriched in the finer fractions (Gu, 1999; Muhs and Bettis, 2000; Peng and Guo, 2001). Thus, sedimentary sorting would lead a decrease in the value of the $SiO_2/$

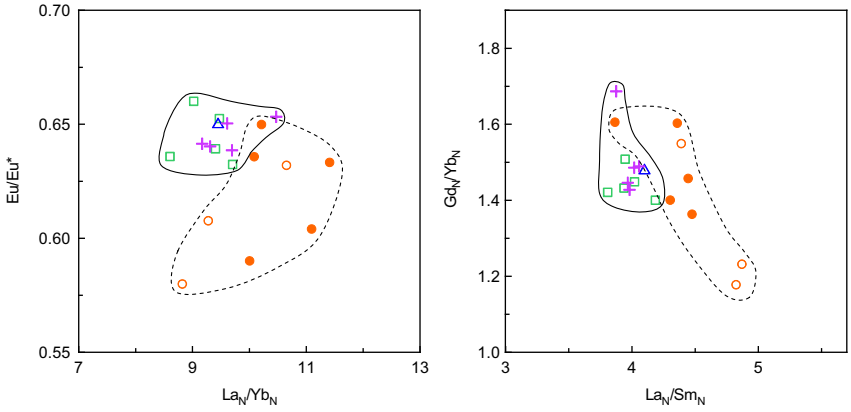

Fig. 4. Plots of parameters of rare earth element (REE) distribution patterns for the <20 μm fraction of loess deposits from Xuancheng in southern China and the CLP in northern China. Symbols are the same as in Fig. 2.

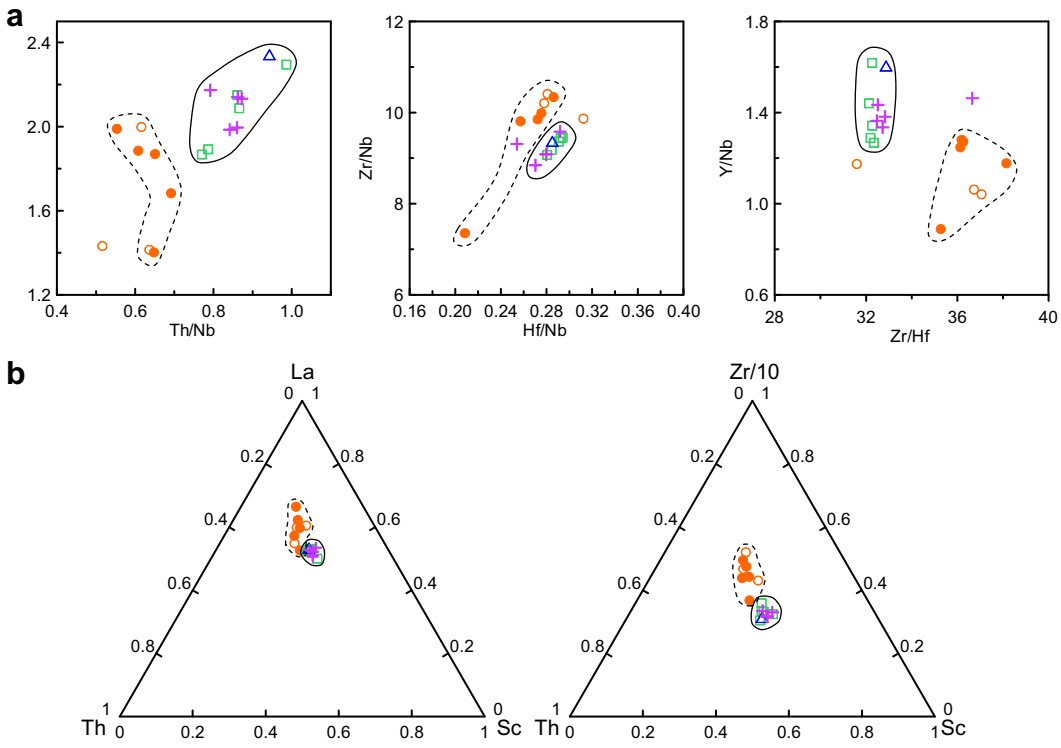

Fig. 5. Plots of immobile trace element ratios (a) and ternary plots of La–Th–Sc and Zr/10-Th–Sc (b) for the <20 μm fraction of loess deposits from Xuancheng in southern China and the CLP in northern China. Symbols are the same as in Fig. 2.

Al_2O_3 ratio with increasing transport distances away from the source area.

The spatial pattern of SiO_2/Al_2O_3 variation is used to test the hypothesis that the southern loess has the same provenance as the loess deposited on the CLP. The SiO_2/Al_2O_3 ratios of the bulk samples from the NW-SE transect on the CLP and from southern China are plotted against latitude in Fig. 7. The generally decreasing trend for the L1LL1 and S1 samples from the CLP indicates the southward decrease in the grain-size of the original particles. However, the SiO_2/Al_2O_3 ratios of samples from XC and FC sections increase sharply. The high SiO_2/Al_2O_3 values (8.66 ± 0.39, $n = 22$) are also seen in another typical *Xiashu* loess section at Dagang (32°13.23′N, 119°41.2′E) (Chen et al., 2008) (Fig. 1c). Any weathering that may have occurred would have led to depletion rather than enrichment in Si. Therefore, the enrichment of SiO_2 in the loess in southern China runs contrary to the concept that the southern loess is derived from northern deserts.

4. Discussion

4.1. Geochemical evidence of a local source for the loess in southern China

This study shows remarkable differences in ratios of relatively immobile major, trace elements and some REE distribution indices, indicating differences in the geochemical composition of source materials for the <20 μm fraction between XC section in southern China and loess on the CLP. As only eolian particles of <20 μm in diameter can be transported over long distances, the compositional differences in the <20 μm fraction suggest that the loess deposits in the two regions have different dust sources. This is also supported by spatial changes in SiO_2/Al_2O_3 values of bulk loess samples in an NW-SE transect. The loess deposits on the CLP derived from deserts in the Asian interior show a southward decreasing trend in SiO_2/Al_2O_3 ratios due to the effects of

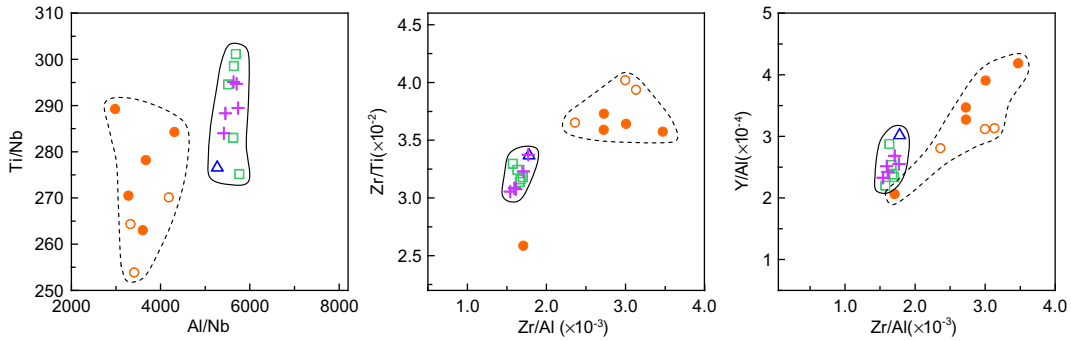

Fig. 6. Plots of immobile elements ratios between trace and major elements for the <20 μm fraction of loess deposits from Xuancheng in southern China and the CLP in northern China. Symbols are the same as in Fig. 2.

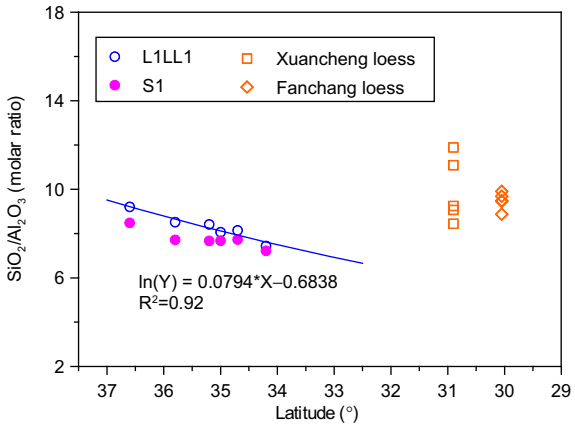

Fig. 7. Spatial changes in SiO_2/Al_2O_3 ratios plotted against latitude for bulk samples from southern China and the CLP. The loess L1LL1 and soil S1 samples on the CLP are from the NW-SE transect of Huanxian, Xifeng, Changwu, Binxian, Yongshou and Lantian, as shown in Fig.. 1b. The solid line is the exponential fit line of the L1LL1samples on the Loess Plateau deposited under glacial climate condition.

sedimentary sorting on particle size. The high SiO_2/Al_2O_3 values of bulk samples from the typical southern loess sections do not lie on this trend.

Compared with the loess deposits from the CLP, the southern ones have a more variable elemental composition, as shown in Figs. 2–6. To investigate differences in chemical composition, we compile the plot of K_2O/Al_2O_3 vs. TiO_2/Al_2O_3 (Fig. 8) for bulk samples from typical sections in the two regions from the published data. Gu (1999) found that K_2O/Al_2O_3 and TiO_2/Al_2O_3 are almost uniform across different grain-size fractions for the silt-sized particles in Chinese loess. Thus, these two ratios, both independent of sedimentary differentiation, can serve to trace the provenance of silt-sized sediments using bulk measurements. Hao (2001) has used a plot of K_2O/Al_2O_3 vs. TiO_2/Al_2O_3 to trace the source of loess of Miocene age.

The southern loess samples and those from the CLP are easily distinguished from one another using a plot of K_2O/Al_2O_3 vs. TiO_2/Al_2O_3 (Fig. 8). This plot demonstrates: (1) roughly identical ranges of TiO_2/Al_2O_3 and K_2O/Al_2O_3 for the loess deposits across the central Loess Plateau, (2) a clear difference in TiO_2/Al_2O_3 values in the loess deposits between southern China and CLP, and (3) a wide range of variation in K_2O/Al_2O_3 and TiO_2/Al_2O_3 values between sites in the lower reaches of the Yangtze River. The roughly identical ranges of K_2O/Al_2O_3 and TiO_2/Al_2O_3 values for Pleistocene loess and Pliocene Red Earth on the CLP suggest that they come from broadly similar desert sources, consistent with previous studies (Guo et al., 2001; Wang et al., 2007; Liang et al., 2009). The bulk samples of Xifeng Red Earth have similar grain-size to the southern loess (Li et al., 1997, 2001; Guo et al., 2001), thus differences in TiO_2/Al_2O_3 between the southern loess and Xifeng Red Earth and Pleistocene loess can only be attributed to difference in dust provenances rather than variations in grain-size. The remarkable variety in TiO_2/Al_2O_3 values between the different sites in southern China suggests a diversity of dust sources. The striking variations in K_2O/Al_2O_3 values between sites in the lower reaches of the Yangtze River may be attributed to both changes in source area and weathering intensity. The Dagang and Xiangyang sections have thicknesses of ~60 and ~10 m, respectively, over a similar age span (Li et al., 1997; Chen et al., 2008). Dagang and Xiangyang have a mean annual precipitation (MAP) of 1100 mm and 1350 mm, respectively, much higher than the MAP of 400–700 mm in the eastern CLP. Under similar climates, the greater rate of loess accumulation at Dagang would lead to a decrease in the duration of exposure and thus, in principle, should result in less chemical weathering, which could explain the different K_2O/Al_2O_3 ratios. Because of the potential mobility of K_2O, K_2O/Al_2O_3 cannot be used as a provenance indicator in silt-sized sediments in humid region, although it can provide some information on the provenance of sediments in higher latitudes, e.g. loess deposits on the CLP, where the weathering profiles have often only experienced an early stage of chemical weathering involving Ca and Na depletion.

In summary, the geochemical evidence indicates that the loess in the lower reaches of the Yangtze River has different sources from the loess on the CLP. Additionally, the variability in chemical composition suggests that the southern loess has multiple source regions. The adjacent regions to the north of Yangtze River are the fluvial floodplains in eastern China,

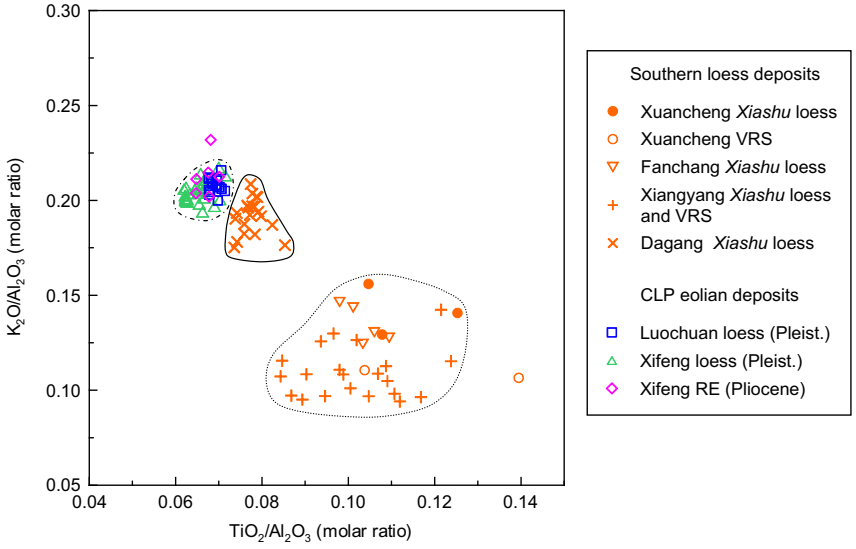

Fig. 8. Plot of of K_2O/Al_2O_3 vs. TiO_2/Al_2O_3 for the bulk samples of the loess deposits in the lower reaches of the Yangtze River in southern China and the CLP in northern China. The data for the Xiangyang and Dagang sections are from Li et al. (1999) and Chen et al. (2008), respectively. Those for the Luochuan section are from Gallet et al. (1996), and for the Xifeng section, from Liang et al. (2009).

comprising mainly the Huaihe River drainage area and a small part of Yangtze River drainage area. There are extensive, shallow overspill lakes on the plains. The dried lake beds, exposed river valley floors and other fine sediments on the fluvial floodplains would have been credible sources for eolian dust particles given a sufficiently dry glacial climate in the region. We infer that the loess deposits in southern China were primarily derived from these sources.

4.2. Role of the East Asian winter monsoon in dust transportation over China

The dust emitted from deserts in the Asian interior has been transported by different patterns of atmospheric circulation and deposited over a wide area. The high-altitude westerlies in the Northern Hemisphere transported the dust to the north Pacific Ocean and formed the latitudinal band of quartz-rich sediments at about 30–40°N (Rex and Goldberg, 1958; Rea, 1994). The low-altitude winds of the East Asian winter monsoon circulation are the predominant carriers for the loess deposits in the CLP, transporting dusts from the Gobi (stony desert) in southern Mongolia and the adjoining Gobi and sand deserts in northern China (Sun, 2002; Sun et al., 2008). That the dominant source lies in the northern deserts is well reflected by the way in which contours of southwardly declining median grain-size lie nearly parallel to the lines of latitude (Nugteren and Vandenberghe, 2004; Yang and Ding, 2008).

The sedimentary differentiation of eolian particles transported by the winds of the East Asian winter monsoon is very rapid, as indicated by the sharp southward decrease in median grain-size (Yang and Ding, 2004) and eolian mass accumulation rates (Kohfeld and Harrison, 2003) in the upper Malan loess (MIS 2). During dust storms, dust concentration decreases sharply with height in accordance with a power function in the atmospheric boundary layer (e.g. Nickling, 1978). The Loess Plateau is bounded by the Qinling Mts. in the south and the Lüliang and Taihang Mts in the east, both reaching elevations ranging from 1000 to over 2000 m, thus forming a barrier to dust transportation. Consequently, the physical constraints on dust transportation, coupled with the topographical barriers are unfavorable to southward transport of silt-sized dusts from northern deserts to southern China.

Sustained dust deposition in the Yangtze River basin started at around 0.85 Ma (Qiao et al., 2003). It is necessary to address the changes of eolian dust accumulation rates over the CLP around this time. Based on previous magnetostratigraphic studies, average dust accumulation rates increased from 7.07 cm/ka between 1.8 and 0.8 Ma to 9.23 cm/ka after 0.8 Ma in the classic Xifeng section (Liu et al., 1988) and from 5.49 cm/ka between 1.8 and 0.8 Ma to 6.80 cm/ka for the classic Luochuan section (Heller and Liu, 1982). These changes represent an increase of 20–30% in dust accumulation rates on the central CLP after the Middle Pleistocene climate transition. The increase in dust deposition rate is the consequence of increases in the aridity of the desert regions, leading to a southward expansion of the deserts (Guo et al., 2004; Ding et al., 2005), and the increased strength of East Asian winter monsoon winds (Xiao and An, 1999). It has been well accepted that the East Asian monsoon strengthened in the Middle Pleistocene as seen from evidence from the CLP (Guo et al., 1993; Xiao and An, 1999). The local sources for the southern loess indicate that strengthened East Asian winter monsoon was not sufficiently energetic to carry substantial quantities of dust from the northern deserts to the middle-lower reaches of the Yangtze River. Therefore, the role of the East Asian winter monsoon in spreading dust from northern deserts to southern China (e.g. Liu, 1985) has often been overestimated.

4.3. Aridification in the southern China during glacial periods

The occurrence of continuous loess deposits requires the existence of dust source areas and of winds strong enough to carry dust particles. The region between the Yangtze River and Qinling Mts. comprises mainly the Huaihe River drainage area and a small part of Yangtze River drainage area. The abundant fine-grained sediments in these floodplains are the potential source material for the southern loess. The local sources of widespread southern loess suggested by this study point to the aridification of local floodplains in the present northern subtropical area during glacial periods.

The aridity in the northern subtropical area started at around 0.85 Ma indicating an important regional environmental event. The timing is consistent with the Middle Pleistocene climate transition. Marine $\delta^{18}O$ records indicate a drastic increase in global ice volume at this boundary coupled with a change in the dominant orbital cycle from 41 ka to 100 ka (Ruddiman et al., 1989). The intensified cooling in the high northern latitudes induced a strengthened winter monsoon by strengthening the Siberia High Cell, leading to a colder and drier climate during glacial periods. The associated retreat of the marginal seas of the West Pacific Ocean also increased continental aridity in the northern subtropical area. According to Wang (1999), during the last glacial maximum, the shore line in the East China and Yellow seas retreated eastward by around 6–7° of longitude. The evidence from the CLP points to a spatial displacement of the rain front of the summer monsoon by over 600 km between the glacial maxima and interglacial optima during the last 0.6 Ma (Hao and Guo, 2005). The decrease in precipitation and in sea level resulted in a decline in the water levels of the rivers and lakes in the northern subtropical area, and consequently led to an enlarged area of exposed river valley and lake bed deposits. Sporopollen analysis on the typical loess layers in *Xiashu* loess section near Nanjing (Fig. 1c) demonstrates that herbaceous pollen dominates the total pollen sum, comprising mainly Compositae and Gramineae, and subordinately *Artemisia* and Chenopodiaceae, and arboreal pollen is mainly of *Pinus*, indicating a relative arid and cold climate (Huang et al., 1988). During glacial periods, the floodplains with sparse vegetation cover would be easily deflated by wind and become the dust providers. The deflated dust particles were carried by strengthened winter winds and deposited in the nearby regions, forming the southern loess in the present northern subtropical area.

5. Conclusions

The Middle Pleistocene loess deposits in the lower reaches of the Yantze River, southern China have distinctly different chemical composition in relative immobile major and trace elements from those on the Chinese Loess Plateau. The difference indicates that the deserts in Asian interior were not the primary sources for the southern loess. The role of the East Asian winter monsoon in transporting dust from northern deserts to southern China has been overestimated in many previous studies proposing that the southern loess were derived from northern deserts. It is suggested that the adjacent floodplains to the north of the Yangtze River are the dominant dust sources of southern loess. The occurrence of sustained eolian deposits in lower reaches of the Yangtze River is an indication both of local aridification and of strengthened winter monsoon activity during glacial periods, in a region experiencing a northern subtropical climate at present. Dust deposition in the lower reaches of the Yangtze River was a regional environmental response to the Middle Pleistocene climate transition at around 0.8 Ma.

Acknowledgements

This study was supported by the Knowledge Innovation Programs of the Chinese Academy of Sciences (KZCX2-YW-Q1-03), National Basic Research Program of China (973 Program) (2010CB950204) and the National Natural Science Foundation of China (projects 40730104 and 40672115). We are grateful to Professor Dan Muhs, an anonymous reviewer and the editor for the constructive comments and suggestions. Thanks are extended to B. Sun and S. Peng for helps in experiments and Z. Gu, L. Wang, and S. Peng for helpful discussions.

References

Barth, M.G., McDonough, W.F., Rudnick, R.L., 2000. Tracking the budget of Nb and Ta in the continental crust. Chemical Geology 165, 197–213.
Bhatia, M.R., Crook, K.A.W., 1986. Trace element characteristics of graywackes and tectonic setting discrimination of sedimentary basins. Contributions to Mineralogy and Petrology 92, 181–193.
Broecker, W.S., Peng, T.H., 1982. Tracers in the Sea. Eldigio Press, New York.
Chen, J., An, Z.S., Liu, L.W., Ji, J.F., Yang, J.D., Chen, Y., 2001. Variations in chemical compositions of the eolian dust in Chinese Loess Plateau over the past 2.5 Ma and chemical weathering in the Asian inland. Science in China, Series D 44, 403–413.
Chen, Y., Li, X., Han, Z., Yang, S., Wang, Y., Yang, D., 2008. Chemical weathering intensity and element migration features of the Xiashu loess profile in Zhenjiang, Jiangsu Province. Journal of Geographical Sciences 18, 341–352.
Cox, R., Lowe, D.R., Cullers, R.L., 1995. The influence of sediment recycling and basement composition on evolution of mudrock chemistry in the southwestern United-States. Geochimica et Cosmochimica Acta 59, 2919–2940.
Deer, W.A., Howie, R.A., Zussman, J., 1966. An Introduction to the Rock Forming Minerals. Longman, London.
Ding, Z.L., Sun, J.M., Yang, S.L., Liu, T.S., 2001. Geochemistry of the Pliocene red clay formation in the Chinese Loess Plateau and implications for its origin, source provenance and paleoclimate change. Geochimica et Cosmochimica Acta 65, 901–913.
Ding, Z.L., Derbyshire, E., Yang, S.L., Sun, J.M., Liu, T.S., 2005. Stepwise expansion of desert environment across northern China in the past 3.5 Ma and implications for monsoon evolution. Earth and Planetary Science Letters 237, 45–55.
Fralick, P.W., Kronberg, B.I., 1997. Geochemical discrimination of clastic sedimentary rock sources. Sedimentary Geology 113, 111–124.
Galan, E., Fernandez-Caliani, J.C., Miras, A., Aparicio, P., Marquez, M.G., 2007. Residence and fractionation of rare earth elements during kaolinization of alkaline peraluminous granites in NW Spain. Clay Minerals 42, 341–352.
Gallet, S., Jahn, B.M., Torii, M., 1996. Geochemical characterization of the Luochuan loess-paleosol sequence, China, and paleoclimatic implications. Chemical Geology 133, 67–88.
Gallet, S., Jahn, B.M., Lanoe, B.V.V., Dia, A., Rossello, E., 1998. Loess geochemistry and its implications for particle origin and composition of the upper continental crust. Earth and Planetary Science Letters 156, 157–172.
Gouveia, M.A., Prudencio, M.I., Figueiredo, M.O., Pereira, L.C.J., Waerenborgh, J.C., Morgado, I., Pena, T., Lopes, A., 1993. Behavior of REE and other trace and major elements during weathering of granitic rocks, Evora, Portugal. Chemical Geology 107, 293–296.
Gu, Z., 1999. Weathering Histories of Chinese Dust Deposits Based on Uranium and Thorium Series Nuclides, Cosmogenic ^{10}Be, and Major Elements. Ph.D. Thesis, Institute of Geology and Geophysics, Chinese Academy of Sciences, Beijing, China (in Chinese, with English Abstr.).
Guan, Q., Pan, B., Gao, H., Li, N., Zhang, H., Wang, P., 2008. Geochemical evidence of the Chinese loess provenance during the Late Pleistocene. Palaeogeography, Palaeoclimatology, Palaeoecology 270, 53–58.
Guo, Z., Liu, D.S., Fedoroff, N., An, Z.S., 1993. Shift of the monsoon intensity on the loess plateau at ca 0.85 Ma. Chinese Science Bulletin 38, 586–591.
Guo, Z., Biscaye, P., Wei, L., Chen, X., Peng, S., Liu, T., 2000. Summer monsoon variations over the last 1.2 Ma from the weathering of loess-soil sequences in China. Geophysical Research Letters 27, 1751–1754.
Guo, Z.T., Peng, S.Z., Hao, Q.Z., Biscaye, P.E., Liu, T.S., 2001. Origin of the Miocene-Pliocene red-earth formation at Xifeng in northern China and implications for paleoenvironments. Palaeogeography, Palaeoclimatology, Palaeoecology 170, 11–26.
Guo, Z.T., Peng, S.Z., Hao, Q.Z., Biscaye, P.E., An, Z.S., Liu, T.S., 2004. Late Miocene-Pliocene development of Asian aridification as recorded in an eolian sequence in northern China. Global and Planetary Change 41, 135–145.
Hao, Q., 2001. A Stratigraphical Study on the Late Tertiary Eolian Deposit in Western Loess Plateau, Northern China. Ph.D. Thesis, Institute of Geology and Geophysics, Chinese Academy of Sciences, Beijing, China (in Chinese, with English Abstr.).
Hao, Q., Guo, Z., 2004. Magnetostratigraphy of a late Miocene-Pliocene loess-soil sequence in the western Loess Plateau in China. Geophysical Research Letters 31, L09209. doi:10.1029/2003GL019392.
Hao, Q., Guo, Z., 2005. Spatial variations of magnetic susceptibility of Chinese loess for the last 600 kyr: implications for monsoon evolution. Journal of Geophysical Research 110, B12101,. doi:10.1029/2005JB003765.
Heller, F., Liu, T.-S., 1982. Magnetostratigraphical dating of loess deposits in China. Nature 300, 431–433.
Holland, H., 1978. The Chemistry of the Atmosphere and Oceans. John Wiley & Sons, New York.
Hsü, C.S., 1936. Gastropods from the Siashu formation. Palaeontologia Sinica Series B 6, 1–50.
Huang, J.N., Fang, J.Y., Shao, J.J., 1988. Study on the chronology of Xiashu loess in Nanjing area. Geological Review 34, 241–246 (in Chinese, with English Abstr.).
Jahn, B.M., Gallet, S., Han, J.M., 2001. Geochemistry of the Xining, Xifeng and Jixian sections, Loess Plateau of China: eolian dust provenance and paleosol evolution during the last 140 ka. Chemical Geology 178, 71–94.
Kahmann, J.A., Seaman, J., Driese, S.G., 2008. Evaluating trace elements as paleoclimate indicators: multivariate statistical analysis of late Mississippian Pennington Formation paleosols, Kentucky, USA. Journal of Geology 116, 254–268.
Kohfeld, K.E., Harrison, S.P., 2001. DIRTMAP: the geological record of dust. Earth-Science Reviews 54, 81–114.
Kohfeld, K.E., Harrison, S.P., 2003. Glacial-interglacial changes in dust deposition on the Chinese Loess Plateau. Quaternary Science Reviews 22, 1859–1878.
Kohfeld, K.E., Tegen, I., 2007. Record of mineral aerosols and their role in the Earth system. In: Holland, H.D., Turekian, K.K. (Eds.), Treatise on Geochemistry. Elsevier, New York, pp. 1–26.
Kurtz, A.C., Derry, L.A., Chadwick, O.A., Alfano, M.J., 2000. Refractory element mobility in volcanic soils. Geology 28, 683–686.
Li, X.S., Yang, D.Y., Lu, H.Y., Han, H.Y., 1997. The grain-size features of Quaternary aeolian-dust deposition sequence in south Anhui and their significance. Marine Geology & Quaternary Geology 17, 73–81 (in Chinese, with English Abstr.).
Li, X.S., Yang, D.Y., Lu, H.Y., 1999. Oxide-geochemistry features and paleoclimatic record of the aeolian-dust depositional sequence in southern Anhui. Marine Geology & Quaternary Geology 19, 75–82 (in Chinese, with English Abstr.).
Li, X.S., Yang, D.Y., Lu, H.Y., 2001. Grain-size features and genesis of the Xiashu loess in Zhenjiang. Marine Geology & Quaternary Geology 21, 25–32 (in Chinese, with English Abstr.).
Li, Y.H., 2000. A Compendium of Geochemistry: from Solar Nebula to the Human Brain. Princeton Univ Press, Princeton.
Liang, M.Y., Guo, Z.T., Kahmann, A., Oldfield, F., 2009. Geochemical characteristics of the Miocene eolian deposits in China: their provenance and climate implications. Geochemistry Geophysics Geosystems 10, Q04004. doi:10.1029/2008GC002331.
Liu, T., 1985. Loess and the Environment. China Ocean Press, Beijing.
Liu, X., Liu, T., Xu, T., Chen, M., 1988. The Chinese loess in Xifeng, I. The primary study on magnetostratigraphy of a loess profile in Xifeng area, Gansu province. Geophysical Journal of the Royal Astronomical Society 92, 345–348.
Mclennan, S.M., 1989. Rare-earth elements in sedimentary-rocks – influence of provenance and sedimentary processes. Reviews in Mineralogy 21, 169–200.
McLennan, S., Taylor, S., Kroner, A., 1983. Geochemical evolution of Archean shales from South Africa. I: the Swaziland and Pongola supergroups. Precambrian Research 22, 93–124.
McLennan, S.M., Hemming, S., McDaniel, D.K., Hanson, G.N., 1993. Geochemical approaches to sedimentation, provenance and tectonics. In: Johnsson, M.J., Basu, A. (Eds.), Processes Controlling the Composition of Clastic Sediments, pp. 21–40. Boulder, Colorado.
Muhs, D., Bettis, E., 2000. Geochemical variations in Peoria Loess of western Iowa indicate paleowinds of midcontinental North America during last glaciation. Quaternary Research 53, 49–61.
Muhs, D.R., Stafford, T.W., Cowherd, S.D., Mahan, S.A., Kihl, R., Maat, P.B., Bush, C.A., Nehring, J., 1996. Origin of the late Quaternary dune fields of northeastern Colorado. Geomorphology 17, 129–149.
Muhs, D.R., Budahn, J.R., Johnson, D.L., Reheis, M., Beann, J., Skipp, G., Fisher, E., Jones, J.A., 2008. Geochemical evidence for airborne dust additions to soils in Channel Islands National Park, California. Geological Society of America Bulletin 120, 106–126.
Nickling, W., 1978. Eolian sediment transport during dust storms: Slims River valley, Yukon Territory. Canadian Journal of Earth Sciences 15, 1069–1084.
Nugteren, G., Vandenberghe, J., 2004. Spatial climatic variability on the Central Loess Plateau (China) as recorded by grain size for the last 250 kyr. Global and Planetary Change 41, 185–206.
Peng, S., Guo, Z., 2001. Geochemical indicator of original eolian grain size and implications on winter monsoon evolution. Science in China, Series D 44 (Suppl.), 261–266.
Pye, K., 1995. The nature, origin and accumulation of loess. Quaternary Science Reviews 14, 653–667.
Qiao, Y.S., Guo, Z.T., Hao, Q.Z., Wu, W.X., Jiang, W.Y., Yuan, B.Y., Zhang, Z.S., Wei, J.J., Zhao, H., 2003. Loess-soil sequences in southern Anhui Province: magnetostratigraphy and paleoclimatic significance. Chinese Science Bulletin 48, 2088–2093.
Rea, D.K., 1994. The paleoclimatic record provided by eolian deposition in the deep sea: the geologic history of wind. Reviews of Geophysics 32, 159–195.
Reheis, M.C., Budahn, J.R., Lamothe, P.J., 2002. Geochemical evidence for diversity of dust sources in the southwestern United States. Geochimica et Cosmochimica Acta 66, 1569–1587.
Rex, R., Goldberg, E., 1958. Quartz contents of pelagic sediments of the Pacific Ocean. Tellus 10, 153.

Ruddiman, W., Raymo, M., Martinson, D., Clement, B., Backman, J., 1989. Pleistocene evolution: northern hemisphere ice sheets and North Atlantic Ocean. Paleoceanography 4, 353–412.

Sheldon, N.D., Tabor, N.J., 2009. Quantitative paleoenvironmental and paleoclimatic reconstruction using paleosols. Earth-Science Reviews 95, 1–52.

Shi, Y., Zhang, W., Dai, X., Song, Z., Yu, L., Zheng, X., 2005. Characteristics of clay mineral assemblage of Xiashu Loess and their paleoenvironmental significance. Marine Geology & Quaternary Geology 25, 99–105 (in Chinese, with English Abstr.).

Sugitani, K., Horiuchi, Y., Adachi, M., Sugisaki, R., 1996. Anomalously low Al_2O_3/TiO_2 values for Archean cherts from the Pilbara Block, Western Australia–possible evidence for extensive chemical weathering on the early earth. Precambrian Research 80, 49–76.

Sun, J., 2002. Provenance of loess material and formation of loess deposits on the Chinese Loess Plateau. Earth and Planetary Science Letters 203, 845–859.

Sun, Y., Tada, R., Chen, J., Liu, Q., Toyoda, S., Tani, A., Ji, J., Isozaki, Y., 2008. Tracing the provenance of fine-grained dust deposited on the central Chinese Loess Plateau. Geophysical Research Letters 35, L01804. doi:10.1029/2007GL031672.

Taylor, S.R., McLennan, S.M., 1985. The Continental Crust: Its Composition and Evolution. Blackwell, Oxford.

Tsoar, H., Pye, K., 1987. Dust transport and the question of desert loess formation. Sedimentology 34, 139–153.

Wang, P.X., 1999. Response of Western Pacific marginal seas to glacial cycles: paleoceanographic and sedimentological features. Marine Geology 156, 5–39.

Wang, Y.X., Yang, J.D., Chen, J., Zhang, K.J., Rao, W.B., 2007. The Sr and Nd isotopic variations of the Chinese loess plateau during the past 7 Ma: implications for the east Asian winter monsoon and source areas of loess. Palaeogeography, Palaeoclimatology, Palaeoecology 249, 351–361.

Wu, S.G., Chen, Y.Y., Yang, D.Y., 1992. A preliminary study on the "Xiashu" clay in Zhenjiang, Jiangsu. In: Liu, T.S., An, Z.S. (Eds.), Loess, Quaternary Geology and Global Change, III. Science Press, Beijing, pp. 122–127 (in Chinese).

Xiao, J., An, Z., 1999. Three large shifts in East Asian monsoon circulation indicated by loess-paleosol sequences in China and late Cenozoic deposits in Japan. Palaeogeography, Palaeoclimatology, Palaeoecology 154, 179–189.

Xie, S., Lai, X., Yi, Y., Gu, Y., Liu, Y., Wang, X., Liu, G., Liang, B., 2003. Molecular fossils in a Pleistocene river terrace in southern China related to paleoclimate variation. Organic Geochemistry 34, 789–797.

Yang, D., Han, H., Zhou, L., Fang, Y., 1991. Eolian deposit and environmental change of middle-late Pleistocene in Xuancheng, Anhui Province south of the lower reaches of the Changjiang River. Marine Geology & Quaternary Geology 11, 97–104 (in Chinese, with English Abstr.).

Yang, S., Ding, Z., 2004. Comparison of particle size characteristics of the Tertiary 'red clay' and Pleistocene loess in the Chinese loess plateau: implications for origin and sources of the 'red clay'. Sedimentology 51, 77–93.

Yang, S., Ding, Z., 2008. Advance–retreat history of the East-Asian summer monsoon rainfall belt over northern China during the last two glacial–interglacial cycles. Earth and Planetary Science Letters 274, 499–510.

Yang, S.Y., Li, C.X., Yang, D.Y., Li, X.S., 2004. Chemical weathering of the loess deposits in the lower Changjiang Valley, China, and paleoclimatic implications. Quaternary International 117, 27–34.

Yang, X., Liu, Y., Li, C., Song, Y., Zhu, H., Jin, X., 2007a. Rare earth elements of aeolian deposits in Northern China and their implications for determining the provenance of dust storms in Beijing. Geomorphology 87, 365–377.

Yang, X., Zhu, B., White, P., 2007b. Provenance of aeolian sediment in the Taklamakan Desert of western China, inferred from REE and major-elemental data. Quaternary International 175, 71–85.

Zhang, W.G., Yu, L.Z., Lu, M., Zheng, X.M., Shi, Y.X., 2007. Magnetic properties and geochemistry of the Xiashu Loess in the present subtropical area of China, and their implications for pedogenic intensity. Earth and Planetary Science Letters 260, 86–97.

Zhang, W.G., Yu, L.Z., Lu, M., Zheng, X.M., Ji, J.F., Zhou, L.M., Wang, X.Y., 2009. East Asian summer monsoon intensity inferred from iron oxide mineralogy in the Xiashu Loess in southern China. Quaternary Science Reviews 28, 345–353.

Zhao, Q.G., Yang, H., 1995. A preliminary study of red earth and changes of Quaternary environment in South China. Quaternary Science (2), 107–116 (in Chinese, with English Abstr.).